

2D-3D Correspondence in Mammography

Robert Martí^{a*}, Reyer Zwiggelaar^{a†}, Caroline Rubin^b and Erika Denton^c

^aSchool of Information Systems, University of East Anglia, Norwich NR4 7TJ, UK

^bBreast Screening Unit, Royal South Hants Hospital, Southampton, UK

^cDepartment of Breast Imaging, Norfolk and Norwich University Hospital, Norwich, UK

Abstract. The fusion of various images obtained from non-rigid deformed objects is discussed. We present a framework for the fusion of multi-modal medical images and we show its application to registration and correspondence of mammographic MR (3D data) and X-ray (2D data) images. The robustness of the presented work relies on the development of a novel method to establish non-linear correspondence between modalities of different dimensionality, which also represent different physical tissue aspects. The correspondence is based on a matching process, which takes into account features from internal linear structures from both images. Initial quantitative and qualitative evaluation results are given which indicate the validity of our approach.

1 Introduction

This work presents a methodology for correspondence of mammographic MR and X-ray images. X-ray mammography is the common modality used for breast cancer screening. A 2D image is generated of the compressed breast. It provides accurate morphological information which allows visualisation of abnormalities which are too small to detect in physical examinations. MR images provide both morphological (tissue distribution) and functional (dynamic studies) information and often are used to complement X-ray mammographic information to provide a more specific diagnosis. In this case a 3D image is obtained from a set of slices and in general no breast compression is used. Examples of both modalities are shown in Fig. 1.

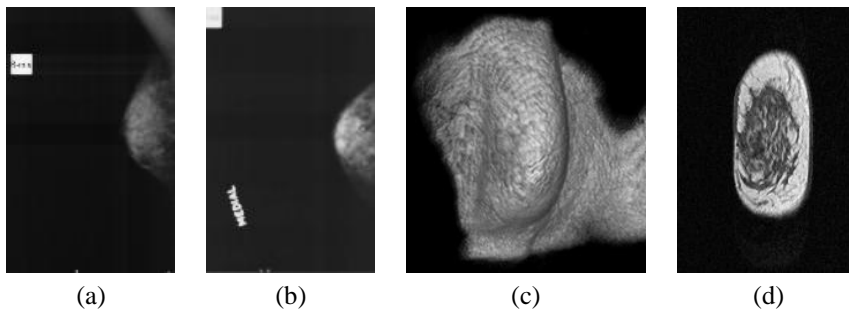


Figure 1. Various modalities: X-ray (a) MLO and (b) CC views, (c) MR surface rendering and (d) MR slice.

We present a novel method to establish correspondence between X-ray and MR breast images. This involves 2D-3D correspondence, which we subdivide into a 2D X-ray to 2D MR projection and 2D MR projection to 3D MR volume correspondence. For both correspondence problems a similar approach is used which is based on matching salient points along internal linear structures [1]. Initially a projection of the MR volume is generated which simulates the X-ray view (see Sec. 2). Subsequently, the 2D images are registered matching their most significant linear structures (see Sec. 3). Using this correspondence, matched points from the projection image are tracked back to the MR volume, thus obtaining a correspondence between the 2D X-ray image and the 3D MR volume (see Sec. 4).

2 MR Projection Image

We aim to obtain an X-ray like image from the projected MR volume in order to match a particular X-ray view. An example of a MR volume is shown in Fig. 1c. The first step in the generation of the projection is to rotate the volume to match the X-ray view of interest. Generally three different views are common: cranio-caudal (CC), medio-lateral (ML) and medio-lateral oblique (MLO). Fig. 1a,b shows examples of such views. In order to obtain a more realistic image we simulate the X-ray imaging process using the MR data. This takes into account the thickness of the volume and the anatomical characteristics of the tissue. The latter is represented by the attenuation coefficient (μ) of the tissue and its density (ρ). Depending of the type of tissue different attenuation coefficients are

* Corresponding author, e-mail: marti@sys.uea.ac.uk

† e-mail: rz@sys.uea.ac.uk

used. Therefore an initial segmentation of the 3D volume should be obtained. Basically, three main regions can be observed in a MR breast image: background, fatty and glandular tissue, as shown in the MR slice in Fig. 1d. Our approach uses the Expectation Maximisation (EM) algorithm [2], in combination with a 3D region growing algorithm, to segment the MR volume into three classes. Subsequently, a projection image is generated using a simple X-ray model with different attenuation coefficients for each region in the segmented volume.

$$I = I_0 \exp(-(\mu_{fa}/\rho_{fa})x_{fa}) - (\mu_{gl}/\rho_{gl})x_{gl}) \quad (1)$$

where I_0 is the incident energy, μ_{fa} and μ_{gl} are the attenuation coefficients of fatty and glandular tissues respectively, ρ_{fa} and ρ_{gl} are their densities and x_{fa} and x_{gl} their thicknesses. Typical values of μ/ρ are tabulated for different elements and compounds and various energy ranges [3]. Fig. 2b shows an MLO projection image obtained using this model.

3 Correspondence Method

Once the projection image has been obtained, it is matched to the X-ray image it aims to simulate. The correspondence method is based on matching salient points from linear structures. This is based on previous work [1] where it has been successfully used for the correspondence between the same views of X-ray mammographic images from the same patient. We use a non-linear line operator [4] to detect linear structures in both images. A multi-scale implementation of the non-linear line operator provides line strength, orientation and scale at a pixel level. The main aim of is to extract characteristic points of linear structures determined by their maximal curvature within a local neighbourhood. Position, orientation and width features are then extracted from those points and used to find correspondence with points in the other image. The correspondence is implemented using a distance matrix structure, where each position in the matrix describes a normalised similarity (where lower values mean greater similarity) between features from points in both images. The extraction of distances smaller than a given threshold will obtain a set of potentially matched points. It should be noted that only the best matches are used, leaving the remaining points unmatched. To be able to correlate point positions in both images, an initial global alignment using a similarity transformation (rotation, translation and scaling) and mutual information (MI) is used. Figure 2 shows an example of the X-ray to MR projection correspondence, resulting in a set of matched points.

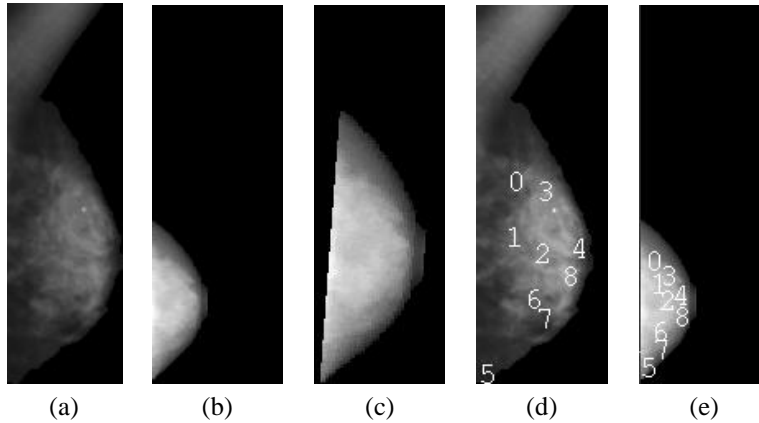


Figure 2. X-ray to MR projection: (a) reference (X-ray image) (b) target (MR projection) images and (c) initial global alignment with MI of (b) to match (a). Matched points are shown in (d) reference and (e) target images.

4 From Projection to Volume

Correspondence points obtained in the 2D registration are used to find the MR slices that are more likely to have generated such points. This can be thought of as another matching process but now matching 2D and 3D points. However, the methodology remains the same as described previously. Salient points in each slice from the MR volume are obtained using the feature extraction process described earlier. A 2D point will be likely to have been generated by a 3D point if the distance as defined in the correspondence process is a local minimum. The z component is discarded from the position feature in the 3D point due to the nature of the matching. Fig. 3 shows an example of such matching: a point in the X-ray image is matched to a point in the MR volume.

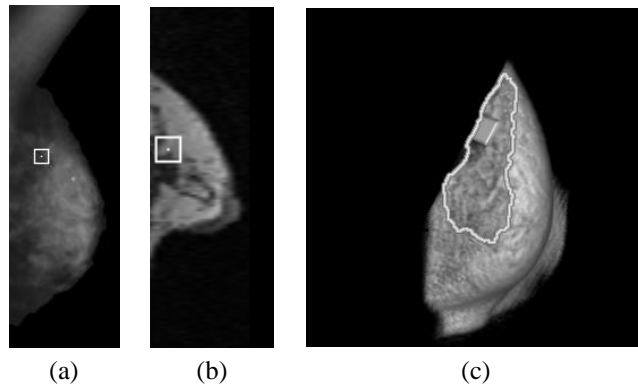


Figure 3. Example of X-ray to MR correspondence: a point from (a) the X-ray image is matched to a point in the MR volume seen here as (b) a single slice and (c) a rendered volume. In all three cases the corresponding point is at the centre of the square.

5 Evaluation Results

In this section evaluation of the proposed methodology and initial results for the correspondence of X-ray and MR data obtained from the same patient are presented. The projection image is generated with the aim to emulate its corresponding X-ray view. As various projection images could be obtained depending on the transformation angles a test was performed to determine an optimum projection angle which maximised the similarity between the projection and the X-ray images. The mutual information between X-ray and projection images obtained under different projection angles (from 0° to 50° with respect to the x axes) was measured. As seen in Fig. 4 a maximum is obtained around 30 degrees which lies inside the angle range for an MLO view. It should be noted that this optimum angle is image dependent and will vary for different X-ray images.

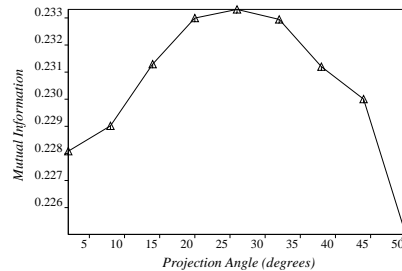


Figure 4. Evaluation of the 2D X-ray to 2D MR projection correspondence: Similarity measures (MI) obtained for various MR projection angles.

Once 2D correspondence between the projection and the X-ray is obtained, points from the projection image are tracked back to the MR volume. We investigated the correlation between features from the (2D) MR projection image and the (3D) MR volume. A linear correlation between features is to be expected, although some uncertainty is introduced caused by the loss of information when the MR projection is generated. Fig. 5 plots the different features extracted from matched points from the MR volume and the projection image (at 30°). A clear linear correlation is obtained for the position and width measures, but this correlation is less obvious for the orientation. For all three cases a linear approximation has been included which shows the expected behaviour.

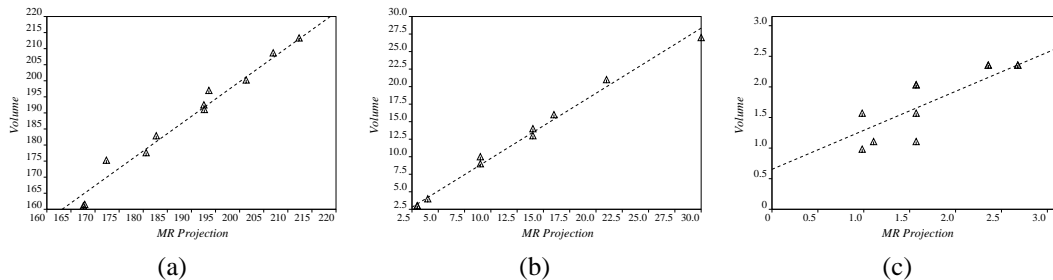


Figure 5. Evaluation of the 2D MR projection to 3D MR volume correspondence. Features from both projection and MR volume: (a) position, (b) width and (c) orientation.

The robustness of the proposed approach is assessed by observing the correspondence results between the X-ray

and projection images where a range of projection angles close to the most likely projection angle (see Fig. 4) were used. The results of this evaluation can be found in Fig. 6, which shows an example of a good and a bad match. To obtain each graph a single salient point from the X-ray image has been used. For each projection angle a matched point in the MR volume is shown described by its slice number. For a robust correspondence point (see Fig. 6a) the resulting slices show little variation as a function of the projection angle and it should be noted that corresponding points have been found for all projection angles. We believe that the apparent oscillation is due to the volume interpolation used for the generation of each projection image but this will need further investigation. For a less robust correspondence point (see Fig. 6b) two changes occur. Firstly, the variation in the resulting slice increases which means that it becomes less certain to which slice the X-ray point should be matched. Secondly, it should be clear that for certain projection angles no matches have been found. It should be mentioned that the less robust point used to generate Fig. 6b is not part of the final points found by the matching process. We believe that an improvement in the quality (i.e. the resolution) of the MR data would provide a shift towards more robust correspondence points.

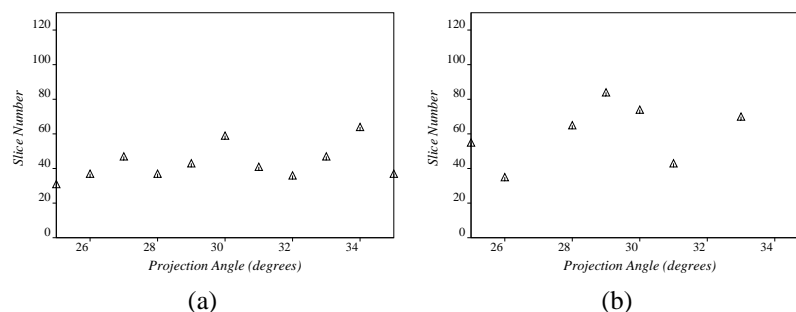


Figure 6. Evaluation of the 2D X-ray to 3D MR volume correspondence: slice correspondence for various projection images (from 25 to 35 degrees) using two different points.

6 Discussion and Conclusions

The novelty of this work is the development of a correspondence methodology based on the similarity between linear structures. Correspondence is only based on matching salient anatomical structures found in both images, therefore in principle, differences due to the presence of abnormalities or severe structural changes are not used in the correspondence. This latter aspect can be seen as a drawback of methods based on similarity measures, which use the complete image (inclusive any abnormalities when present) to obtain correspondence. Although effects related to breast compression are not investigated here, it is our belief that the non-rigid registration between the X-ray image and the MR projection volume (shown in Fig. 2) indirectly accounts for some of those differences.

The results presented are based on a small image database. The size of the database is a reflection on the difficulty to obtain the X-ray and MR images from the same patient at approximately the same time. We believe that better results will be obtained when the quality of the data is improved and the size of the database is enlarged. However, it should be mentioned that throughout the development no database related assumptions have been made. One of the most difficult problems we encountered in the presented work was its evaluation. Quantitative and qualitative methods have been proposed which indicate the validity of our approach. However, it could be argued that other evaluation approaches could be used; for instance the evaluation by an expert radiologist. Initially we want to avoid such a subjective approach, but this will be part of the final evaluation stage of the developed method.

Acknowledgements

This work was supported by EPSRC grant GR/M53387, "Multi-Modality Mammography".

References

1. R. Marti, R. Zwiggelaar & C. Rubin. "Automatic mammographic registration: towards the detection of abnormalities." In *5th Conference on Medical Image Understanding and Analysis*, pp. 149–152. 2001.
2. P. Demster, N. Laird & D. Rubin. "Maximum likelihood from incomplete data via the EM algorithm." *Journal of the Royal Statistical Society B* **39**, pp. 1–38, 1977.
3. J. Hubbell & S. Seltzer. "Tables of X-ray mass attenuation coefficients and mass energy-absorption coefficients." Technical report, National Institute of Standards and Technology, Gaithersburg, MD, 1997. <http://physics.nist.gov/xaamdi>.
4. R. Dixon & C. Taylor. "Automated asbestos fibre counting." *Inst. Phys. Conf. Ser* **44**, pp. 178–185, 1979.